Vol. 493: 57–69, 2013
doi: 10.3354/meps10532

MARINE ECOLOGY PROGRESS SERIES
Mar Ecol Prog Ser

Published November 20

Nutrient pulse induces dynamic changes in cellular C:N:P, amino acids, and paralytic shellfish poisoning toxins in *Alexandrium tamarense*

Dedmer B. Van de Waal[1,2,*], Urban Tillmann[3], Mingming Zhu[3], Boris P. Koch[3,4], Björn Rost[2], Uwe John[3]

[1]Department of Aquatic Ecology, Netherlands Institute of Ecology, PO Box 50, 6700 AB Wageningen, The Netherlands
[2]Marine Biogeosciences and [3]Ecological Chemistry, Alfred-Wegener-Institut Helmholtz-Zentrum für Polar- und Meeresforschung, Am Handelshafen 12, 27570 Bremerhaven, Germany
[4]University of Applied Sciences, An der Karlstadt 8, 27568 Bremerhaven, Germany

ABSTRACT: *Alexandrium tamarense* is a common harmful algal bloom species that can cause high concentrations of paralytic shellfish poisoning toxins (PSTs) in marine coastal waters. PSTs are nitrogen-rich alkaloids, and their production has been shown to depend on resource conditions as well as on growth rate. We hypothesized that PST content in *A. tamarense* depends on the nitrogen availability and will increase with cellular N:P ratios and arginine content. To test this hypothesis, we first grew *A. tamarense* cells under nitrogen-starved, phosphorus-starved and nutrient-replete conditions. Subsequently, we transferred cells into a nutrient-rich medium and followed dynamic changes in growth, elemental stoichiometry, as well as amino acid and PST content and composition. Our results illustrate that PST content was lowest under nitrogen starvation, intermediate under nutrient-replete conditions, and highest under phosphorus starvation. As expected, PST content correlated well with cellular N:P ratios and arginine content. Upon transfer of cells into a nutrient-replete medium, PST content varied with growth rate, depending on the growth-controlling resource. Specifically, PST content increased with growth when recovering from nitrogen starvation and decreased with growth when recovering from phosphorus starvation. Furthermore, PST composition shifted towards less hydroxylated analogues upon resumption of growth. Our findings also illustrate a high potential for luxury consumption of phosphorus by *A. tamarense*. The applied comprehensive approach will help to further elucidate the intriguing coupling between carbon, nitrogen and phosphorus assimilation and the synthesis of amino acids and PSTs.

KEY WORDS: Harmful algal bloom · C:N:P stoichiometry · PSP toxins · Amino acids · *Alexandrium tamarense*

INTRODUCTION

Nutrient concentrations in marine ecosystems have dramatically increased as result of anthropogenic eutrophication (Nixon 1995, Smith et al. 1999). This often leads to the proliferation of harmful algal blooms (HABs) that may cause mass mortalities of fish, illness and death of marine mammals, seabirds, and humans (Granéli & Turner 2006, Anderson et al. 2012b). In marine coastal waters, HABs are commonly produced by dinoflagellates from which the genus *Alexandrium* is among the most prominent with respect to its diversity and global distribution (Anderson et al. 2012a). Moreover, *Alexandrium*

*Email: d.vandewaal@nioo.knaw.nl

blooms are often responsible for the outbreak of paralytic shellfish poisoning (PSP), which is caused by the neurotoxin saxitoxin and its analogues (Shimizu 1996, Cembella 1998).

PSP toxins (PSTs) are nitrogen-rich alkaloids produced by a variety of *Alexandrium* species, including *A. tamarense* (Cembella 1998, Anderson et al. 2012a). Being nitrogen-rich compounds, it is not surprising that PST production has been shown to rely on the relative availability of nitrogen. More specifically, the cellular PST content seems to increase upon phosphorus limitation and decrease upon nitrogen limitation (Boyer et al. 1987, Anderson et al. 1990a,b, Flynn et al. 1994, Béchemin et al. 1999, John & Flynn 1999, 2000). Because cellular N:P ratios typically increase due to phosphorus limitation and decrease upon nitrogen limitation, PST content in *Alexandrium* often correlates well with cellular N:P ratios, especially when grown under nutrient-limiting conditions (Leong et al. 2004, Granéli & Flynn 2006, Lim et al. 2010, Murata et al. 2012). When not limited by nutrients, PST production has been associated with the cell cycle (Taroncher-Oldenburg et al. 1997) and was shown to either increase or decrease with growth rate depending on the growth-controlling environmental factor (Anderson et al. 1990a,b, Cembella 1998, Parkhill & Cembella 1999). Little is yet known about the temporal responses of *Alexandrium* to a nutrient pulse with respect to growth, C:N:P stoichiometry, amino acid synthesis and the content and composition of PSTs.

The dependence of toxin production on nitrogen availability was also found for nitrogen-rich microcystins in the cyanobacterium *Microcystis*, which increased with cellular N:C ratios (Van de Waal et al. 2009). Microcystins comprise up to 89 variants that differ with respect to 2 amino acid positions (Welker & von Döhren 2006). Common amino acids incorporated are leucine, arginine and tyrosine (Sivonen & Jones 1999). It has been shown that the relative cellular availability of arginine substantially increased by providing a pulse of nitrogen to nitrogen-limited cells, which in turn stimulated the incorporation of arginine into microcystins (Tonk et al. 2008, Van de Waal et al. 2010). Arginine is an important precursor for PSTs (Shimizu et al. 1984), and its cellular content was shown to correlate well with the cellular PST content (Anderson et al. 1990b, Flynn et al. 1996, John & Flynn 2000).

Proliferation of phytoplankton is accompanied by substantial changes in resource availability. For instance, high phytoplankton densities under nutrient-rich conditions may cause light limitation (Huisman et al. 1999) and a substantial perturbation of the carbonate chemistry towards low CO_2 and high pH conditions (Talling 1976, Hansen 2002). Furthermore, phytoplankton may become limited by nutrients, notably nitrogen and phosphorus (Elser et al. 2007). These nutrients can be resupplied by the input of nutrient-rich waters from riverine discharge and from deep waters as the result of mixing induced by storms, upwelling, or frontal systems. As a consequence, nitrogen- and phosphorus-limited or -starved cells are suddenly exposed to high concentrations of these nutrients. Such sudden shifts in nutrient availability may cause substantial changes in phytoplankton C:N:P stoichiometry and in turn may have consequences for the production of toxins (Granéli & Flynn 2006, Van de Waal et al. 2009).

Although many studies have reported on the impact of nitrate and phosphate availability on PST production, only few included PST composition, C:N:P stoichiometry, as well as amino acid composition. Yet, it is such a comprehensive approach that may provide an understanding of processes underlying the production of PSTs. Since PSTs are produced from the nitrogen-richest amino acid arginine, we hypothesize that changes in PST content can be explained by changes in the nitrogen availability and amino acid composition. More specifically, we expect PST content to increase with cellular N:P ratios and arginine content. To test this hypothesis, we grew *Alexandrium tamarense* under nitrogen-starved, phosphorus-starved, and nutrient-replete conditions. Once in stationary phase, we transferred cells to a nutrient-rich medium, thereby simulating a nutrient pulse. Subsequently, we followed the dynamic changes in their cellular C:N:P stoichiometry, amino acid composition, as well as PST content and composition.

MATERIALS AND METHODS

Experimental set-up

The clonal strain *Alexandrium tamarense* Alex2 was originally isolated from the Scottish east coast of the North Sea by micro-capillary isolation of single cells (for details see Alpermann et al. 2009, Tillmann et al. 2009). This strain is characterized by the production of various PST analogues, mainly saxitoxin (STX), neosaxitoxin (NEO), C1+C2, and gonyautoxins (GTX1-4), and by its high allelochemical potency (Tillmann et al. 2009). Cells of *A. tamarense* Alex2 were grown as a batch in 2 l Erlenmeyer flasks with

culture medium that comprised 0.2 µm-filtered (Sartobran 300, Satorius) natural North Sea water, containing 25 µM NO_3^-, 0.5 µM NH_4^+, and 1.0 µM PO_4^{3-}. This seawater was enriched with metals and vitamins following the recipe for K medium (Keller et al. 1987), with modified nutrient additions to yield final concentrations of 625 µM NO_3^- and 37 µM PO_4^{3-}, and without the addition of NH_4^+. All cultures were grown at 15°C on a 16:8 h light:dark cycle and at an incident light intensity of 100 ± 10 µmol photons m^{-2} s^{-1} provided by cool-white fluorescent lamps (90 W, Osram). In the first incubations, cultures were grown under nutrient-limited conditions (for details see Zhu & Tillmann 2012). To achieve nitrogen and phosphorus starvation, initial additions of NO_3^- and PO_4^{3-} were lowered to yield final concentrations of 75 µM (i.e. low nitrogen, LN) and 3 µM (i.e. low phosphorus, LP), respectively. As control, one treatment contained the nutrient-replete modified K medium (i.e. high nitrogen and high phosphorus, HNHP). After stagnant growth in a stationary phase for ~6 d, 25 to 55 ml of each culture were transferred to 1000 ml rich medium that yielded initial population densities of 250 to 350 cells ml^{-1}. In these second incubations, cells were exposed to a sudden nutrient pulse as a result of the transfer of cultures from the LN, LP and HNHP conditions into the nutrient-replete modified K medium, here indicated by a '+' sign (i.e. LN+, LP+ and HNHP+, respectively). Subsequently, cultures were sampled daily or every other day until reaching late exponential growth at population densities of 6000 cells ml^{-1}. All experimental treatments, i.e. both the first and second incubations, were set up in triplicate incubations.

Sampling and analyses

For measurements of NO_3^- and PO_4^{3-} during the first incubations, 30 ml of culture suspension from each replicate was filtered over GF/C filters (Whatman), and samples were stored in plastic flasks at −20°C. Measurements of thawed samples were based on the standard methods of seawater analysis (Grasshoff et al. 1999) via a Continuous Flow Analyser (Evolution III, Alliance) with detection limits of 0.1 and 0.01 µM for NO_3^- and PO_4^{3-}, respectively. pH was measured immediately after sampling with a pH electrode (Schott Instruments), and a 2-point calibration on the NBS scale was applied prior to each measurement.

Population densities were determined by means of duplicate or triplicate counts of 300 to 500 cells per sample with an inverted light microscope (Axiovert 40C). For counting we used 0.2 to 10 ml culture suspension fixed with Lugol's solution (2 % final concentration). Specific growth rates were determined by the intrinsic rate of increase in population densities (Gotelli 1995), and maximum growth rates (μ_{max}) were based on an exponential regression through population densities obtained during the exponential growth phase.

For particulate organic carbon, nitrogen and phosphorus analyses, 10 to 100 ml cell suspension was filtered over precombusted GF/F filters (12 h, 500°C) and stored at −25°C in precombusted glass Petri dishes. Carbon and nitrogen were analyzed on an elemental analyzer (EURO EA3000 series). Prior to phosphorus analyses, filters were oxidized with potassium persulfate for 30 min at 121°C, and phosphorus was analysed colorimetrically in accordance with Hansen & Koroleff (1999). The initial carbon content of cells differed between the treatments, which may be associated with the differences in cell size (Zhu & Tillmann 2012). After transfer into a nutrient-replete medium, the cellular carbon content may correspond to cell size, but it may also represent changes in the synthesis of carbon-rich cellular compounds. Therefore, we expressed the elemental, amino acid and PST contents on a per cell basis.

For analyses of PSTs and amino acids, 1 to 150 ml of culture suspension was filtered over 0.8 µm polycarbonate filters and stored in Eppendorf tubes at −25°C. Thus, extracellular PSTs were excluded and the reported data only includes particulate-bound (i.e. intracellular) PSTs. Prior to analyses of PSTs, cells were re-suspended in 1.2 ml of 0.03 mol l^{-1} acetic acid and lysed for 1 min with a Sonifier 250 ultrasonic probe (Branson Ultrasonics). Samples were transferred into new 1.5 ml reaction vials and centrifuged for 15 min at 10 000 × *g* at 4°C. The supernatant was subsequently transferred into an LC vial and analysed with an Agilent 1100 series HPLC system equipped with fluorescence detection (Agilent), coupled to a PCX 2500 post-column derivatization system (Pickering Laboratories). Separation of analytes was performed on a Phenomenex reversed-phase column (5 µm, C18, 250 × 4.6 mm) equipped with a Phenomenex SecuriGuard pre-column (Krock et al. 2007).

Prior to analyses of amino acids, samples were hydrolyzed with 16 % HCl in the presence of ascorbic acid at 110°C for 24 h. Subsequently, a borate buffer was added to adjust for a constant pH of 9.5 (Fitznar et al. 1999). After derivatization with *o*-phthaldialdehyde and 2-mercaptoethanol (Merck), amino acids

were analysed with an Agilent 1200 Series HPLC system equipped with an autosampler for automatic derivatization and fluorescence detection (Agilent), and a Phenomenex Kinetex column (2.6 µm, C18, 150 × 4.6 mm) with guard column (4 × 3 mm). Glutamic acid (Glu) and aspartic acid (Asp) can be formed during hydrolysis from glutamine (Gln) and asparagine (Asn), respectively. Therefore, these amino acids were pooled and reported as Glx (Glu+Gln), and Asx (Asp+Asn). Amino acid concentrations in the extract were calculated based on a series of standard amino acid analyses (Sigma-Aldrich).

Statistical analyses

Growth, elemental contents and ratios, and PST data were tested for normality using the Shapiro-Wilk test. Significance of differences between treatments was tested using 1-way ANOVA, followed by a Tukey's HSD post hoc test. Variables were log-transformed if this improved the homogeneity of variances, as evaluated by Levene's test ($\alpha = 0.05$; Quinn & Keough 2002). When normality failed, significance of differences between treatments was tested using Kruskal-Wallis 1-way ANOVA on ranks, followed by a Student-Newman-Keuls test. All statistical analyses were performed using Sigmaplot 12.0 (Systat Software).

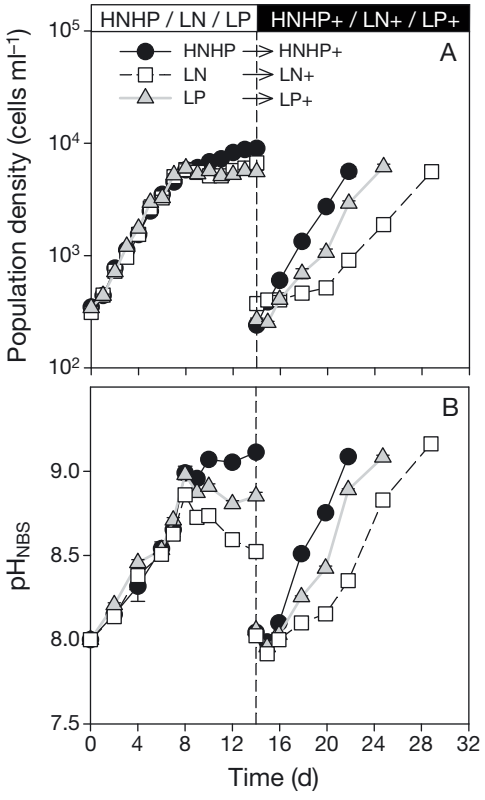

Fig. 1. *Alexandrium tamarense*. Changes (mean ± SE) in (A) population densities and (B) pH in the different treatments prior and after the transfer of cells into a nutrient-replete medium on Day 14 (dashed vertical line) (n = 3). HNHP: high nitrogen and high phosphorus; LN: low nitrogen; LP: low phosphorus. +: nutrient-replete modified K medium

RESULTS

In the first incubations prior to the transfer of cells into a nutrient-replete medium, population densities reached the stationary phase after ~8 d. In the stationary phase, we assumed that LN cultures were starved by nitrogen, LP cultures by phosphorus, and HNHP cultures by inorganic carbon or were affected by the high pH (Fig. 1). The assumption of nitrogen and phosphorus starvation was based on low residual nutrient concentrations (i.e. below detection limit), while nutrient concentrations were in excess in the HNHP treatment. Furthermore, cell growth resumed after the addition of just nitrate or phosphate, suggesting starvation by nitrogen and phosphorus in the LN and LP treatments, respectively (for details see Zhu & Tillmann 2012). In the second incubations after the transfer into a nutrient-replete medium, HNHP+ cultures resumed growth immediately, whereas LN+ and LP+ cultures resumed growth after ~4 and 1 d, respectively. All cultures were grown until they reached the late exponential phase with a population density of 6000 cells ml^{-1} and a pH of 9.1, comparable to the late exponential phase observed in the HNHP treatment prior to nutrient resupply (Fig. 1). Maximum growth rates obtained during the exponential growth phase (Days 0–9) prior to nutrient resupply were similar in all cultures. After nutrient resupply, however, maximum growth rates in the LN+ (Days 18–25) and LP+ (Days 15–25) treatments were 16 and 32% lower as compared to the HNHP+ treatment (Days 14–22) (Table 1; ANOVA, $F_{3,8} = 91.6$, $p < 0.001$).

The cellular carbon content prior to the transfer of cells into a nutrient-replete medium was highest in the LP treatment, containing 50 to 60% more carbon as compared to the HNHP and LN treatments (Fig. 2A, Table 1; ANOVA, $F_{6,14} = 27.8$, $p < 0.001$). Lowest nitrogen content was observed in the LN treatment, containing 51 to 58% less nitrogen as compared to the HNHP and LP treatments (Fig. 2C, Table 1; ANOVA, $F_{6,14} = 49.7$, $p < 0.001$). Similarly,

Table 1. *Alexandrium tamarense*. Maximum growth rate (μ_{max}), carbon, nitrogen and phosphorus content, C:N, N:P, and C:P ratios, and paralytic shellfish poisoning toxins (PST) content in the different treatments and growth phases. Data of the high nitrogen and high phosphorus (HNHP) treatment in the exponential growth phase of the 1st incubation (HNHPexp) was obtained from Day 9 (see also Zhu & Tillmann 2012); data from the HNHP treatment was obtained from Day 14. Data of HNHP+, LN+, and LP+ treatment in the 2nd incubations were obtained from Days 22, 29, and 25, respectively (+: nutrient-replete modified K medium). Values: mean ± SD (n = 3). LN: low nitrogen; LP: low phosphorus. $^{a-e}$Significant differences between treatments and growth phases (ANOVA, $p < 0.001$, followed by Tukey's HSD, $p < 0.05$). *Kruskal-Wallis 1-way ANOVA on ranks, $p < 0.01$, followed by Student-Newman-Keuls test, $p < 0.05$

Treatment	μ_{max} (d^{-1})	C content (pmol $cell^{-1}$)	N content (pmol $cell^{-1}$)	P content (pmol $cell^{-1}$)	C:N ratio (molar)	N:P ratio* (molar)	C:P ratio* (molar)	PST total (fmol $cell^{-1}$)
First incubation, exponential phase								
HNHPexp	0.37 ± 0.01^{a}	181 ± 12^{a}	26.1 ± 2.3^{a}	3.03 ± 0.12^{ab}	7.0 ± 0.2 ^{a}	8.6 ± 0.9^{a}	60 ± 5^{a}	–
First incubation, stationary phase								
HNHP	–	142 ± 6^{b}	20.7 ± 1.1^{a}	2.83 ± 0.14^{ab}	6.8 ± 0.1^{ae}	7.3 ± 0.2^{a}	50 ± 1^{b}	30.3 ± 1.7^{a}
LN	–	132 ± 5^{b}	10.1 ± 0.4^{b}	2.26 ± 0.07^{b}	13.0 ± 0.1^{b}	4.5 ± 0.2^{b}	58 ± 1^{a}	15.8 ± 1.0^{b}
LP	–	211 ± 10^{a}	23.9 ± 1.3^{a}	0.48 ± 0.03^{c}	8.8 ± 0.1^{c}	49.7 ± 2.9^{c}	439 ± 20^{c}	47.3 ± 0.3^{c}
Second incubation, exponential phase								
HNHP+	0.40 ± 0.02^{a}	206 ± 25^{a}	34.0 ± 4.3^{c}	3.25 ± 0.73^{a}	6.1 ± 0.1^{d}	10.8 ± 1.9^{a}	67.6 ± 14.6^{a}	25.9 ± 8.4^{ab}
LN+	0.24 ± 0.01^{b}	252 ± 9^{c}	37.5 ± 1.7^{c}	2.98 ± 0.36^{a}	6.7 ± 0.1^{e}	12.8 ± 2.1^{a}	89.6 ± 13.5^{a}	31.0 ± 4.2^{ac}
LP+	0.32 ± 0.01^{c}	208 ± 20^{a}	34.3 ± 3.0^{c}	2.82 ± 0.31^{ab}	6.1 ± 0.1^{d}	12.2 ± 0.4^{a}	73.9 ± 2.0^{a}	40.4 ± 8.3^{c}

lowest phosphorus content was observed in the LP treatment, containing 83% less phosphorus as compared to the HNHP and LN treatments (Fig. 2E, Table 1; ANOVA, $F_{6,14} = 83.5$, $p < 0.001$). As a consequence of these differences in carbon, nitrogen and phosphorus contents, C:N ratios where highest in the LN treatment, whereas N:P and C:P ratios were highest in the LP treatments (Fig. 2B,D,F, Table 1).

After the transfer into a nutrient-replete medium, the carbon and nitrogen contents, and C:N ratios, converged to comparable values in all treatments (Fig. 2A,B,C, Table 1). Interestingly, nutrient resupply to phosphorus-limited cells caused a considerable initial increase in phosphorus content of over 28-fold within 2 d. After this peak, the phosphorus content gradually decreased towards values similar to the HNHP+ and LN+ treatments (Fig. 2C, Table 1). As a consequence, in the LP+ treatment both the N:P and C:P ratios show an initial decrease from 50 to 5 and 439 to 34, respectively, with a subsequent gradual increase. The N:P and C:P ratios in the HNHP+ and LN+ treatment show an initial increase during the first day after the transfer of cells, which afterwards remains largely unaltered (Fig. 2D,F). The carbon and phosphorus contents, as well as the N:P and C:P ratios, observed at the end of each experiment resemble those observed in the HNHP treatment, whereas the nitrogen content was higher (Table 1).

Upon nutrient starvation, total amino acid content differed substantially between the treatments (Fig. 3). Lowest amounts of cellular amino acids were found in the LN treatment (2.6 ± 0.8 pmol $cell^{-1}$), intermediate amounts were found in the LP treatment (10 ± 0.8 pmol $cell^{-1}$), and highest amounts were found in the HNHP treatment (18 ± 0.1 pmol $cell^{-1}$). After transferring the cultures, amino acid content in the LN+ treatment gradually increased, whereas it showed a drop followed by an increase in the LP+ and HNHP+ treatments until reaching comparable values in all treatments (Fig. 3). The amino acid composition in the different treatments differed upon nutrient starvation. For instance, cellular contents of Glx and arginine were higher in the LP treatment, whereas cellular contents of alanine, serine and glycine were higher in the HNHP treatment. In the LN treatment, all amino acids were present only in low amounts (Fig. 4A). After transferring the cultures, amino acid content in the LN+ treatment increased to comparable values as the LP+ treatment (Fig. 4B). Yet, in the LP+ treatment, cellular contents of valine and leucine were relatively low (0.15 ± 0.06 and 0.31 ± 0.13 pmol $cell^{-1}$, respectively), whereas the glycine content was relatively high (3.55 ± 2.72 pmol $cell^{-1}$). In the HNHP+ treatment, cellular contents of all amino acids, except glycine, showed an increase after nutrient resupply. At the end of each experiment (i.e. at the late exponential growth phase), the amino acid composition in each treatment was comparable (Fig. 4C).

The different treatments resulted in large differences in cellular PST content, which was lowest in the LN treatment (15 ± 1.0 fmol $cell^{-1}$), intermediate in the HNHP treatment (30 ± 1.7 fmol $cell^{-1}$), and highest in the LP treatment (47.3 ± 0.3 fmol $cell^{-1}$;

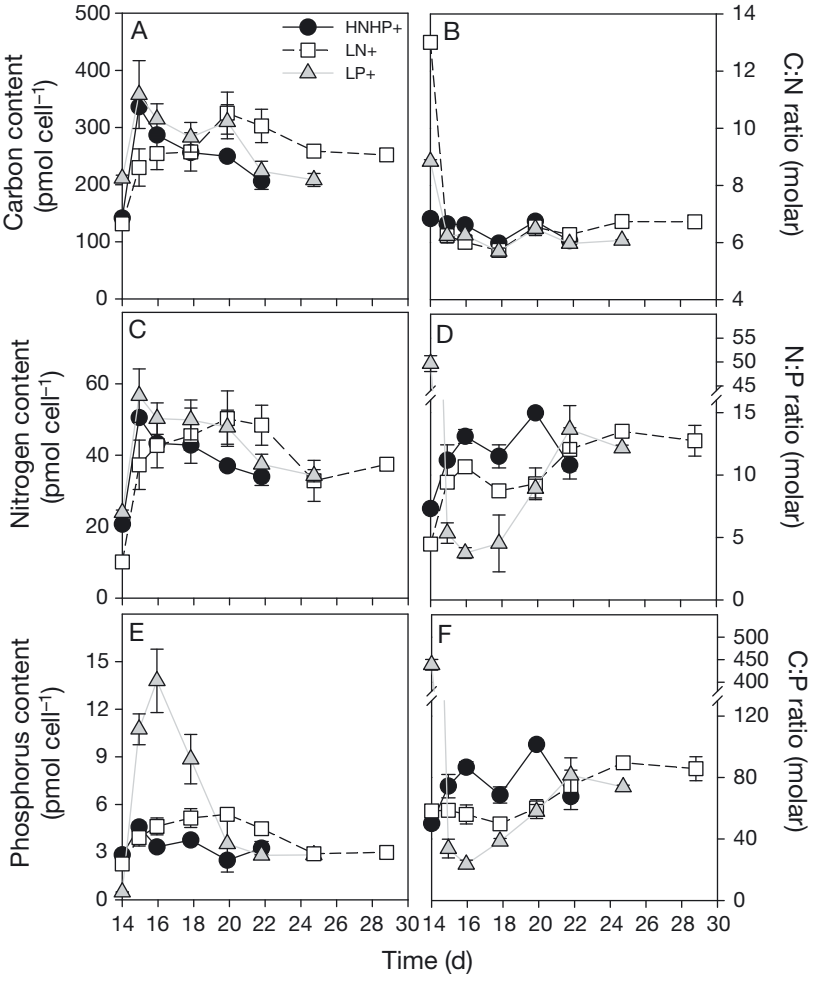

Fig. 2. *Alexandrium tamarense*. Changes (mean ± SE) in cellular (A) carbon, (C) nitrogen and (E) phosphorus contents, and the molar (B) C:N, (D) N:P, and (F) C:P ratios in the different treatments after transfer of cells into nutrient-replete medium on Day 14 (n = 3). See Fig. 1 for definitions

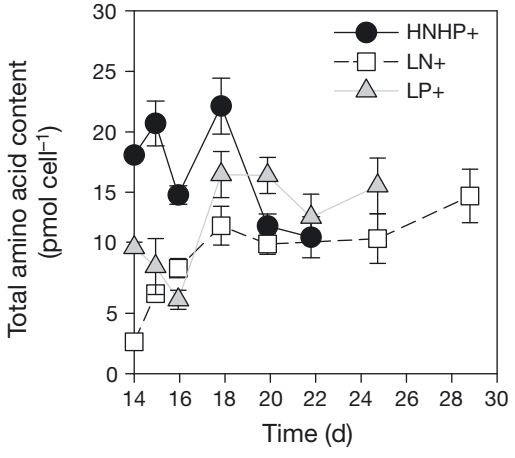

Fig. 3. *Alexandrium tamarense*. Changes (mean ± SE) in total cellular amino acid content in the different treatments after transfer of cells into nutrient-replete medium on Day 14 (n = 3). See Fig. 1 for definitions

Fig. 5, Table 1). After transferring cultures into a nutrient-replete medium, PST content in the HNHP+ treatment remained unaltered, whereas it decreased by 38% in the LP+ treatment (Fig. 5). PST content in the LP+ treatment 4 d after the transfer rapidly increased towards values exceeding those found in the HNHP+ treatment. In the LN+ treatment, PST content gradually increased until reaching comparable values as observed in the HNHP+ treatment (Fig. 5, Table 1). Upon nutrient starvation, PST composition consisted predominately of neosaxitoxin (44–52%), followed by C1+C2 (31–33%), saxitoxin (12–17%) and gonyautoxin 3 and 4 (GTX3+4; 7–13%; Fig. 5, Table 2). After the transfer of cultures into a nutrient-replete medium, the relative contribution of C1+C2 and GTX3+4 remained largely unaltered, whereas the relative contribution of NEO significantly decreased by 7 to 14% (ANOVA, $F_{5,12} = 41.9$, $p < 0.001$) and STX significantly increased by 9 to 14% (Fig. 5, Table 2; ANOVA, $F_{5,12} = 131.4$, $p < 0.001$).

Prior to the transfer of cultures, PST content correlated well with cellular N:P ratios (Fig. 6A, $R^2 = 0.82$, n = 9, $p < 0.001$), and particularly with the cellular arginine content (Fig. 6B, $R^2 = 0.97$, n = 9, $p < 0.001$). After transferring the cultures, growth rates increased and PST content showed differential changes (Fig. 6C). More specifically, PST content increased in the LN+ treatment ($R^2 = 0.97$, n = 24, $p < 0.001$), decreased in the LP+ treatment ($R^2 = 0.28$, n = 21, $p = 0.013$), and remained unaltered in the HNHP+ treatment ($R^2 = 0.04$, n = 18, $p = 0.437$).

DISCUSSION

The resupply of nutrients to starved *Alexandrium tamarense* cells caused substantial changes in their growth, cellular C:N:P stoichiometry, amino acid composition, and cellular PST content. When cells were grown to stationary phase under nutrient-rich conditions in the first incubations, growth presumably became limited by CO_2 or by high pH (Hansen

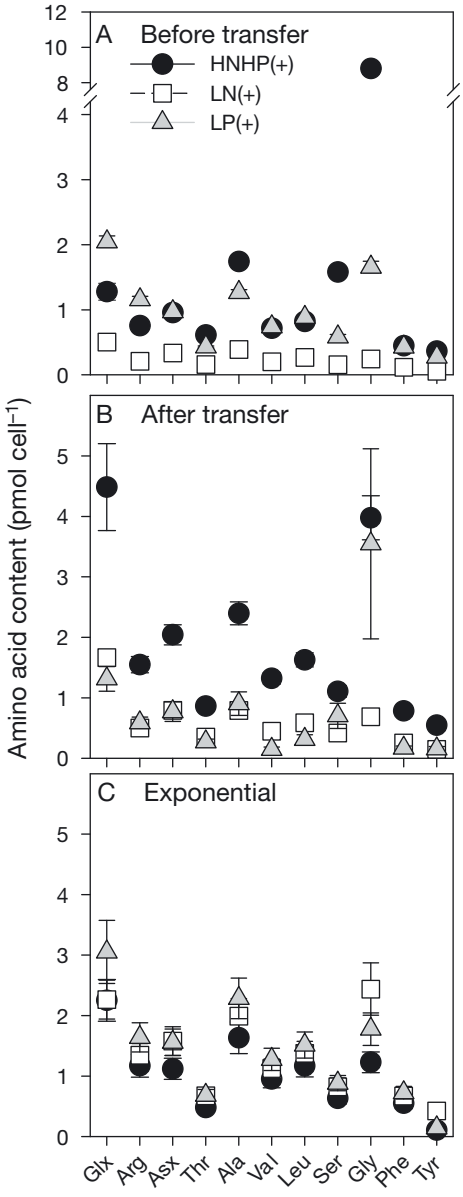

Fig. 4. *Alexandrium tamarense*. Changes (mean ± SE) in cellular amino acid composition (A) prior to, or (B) 1 d after the transfer of cells into nutrient-replete medium, and (C) during the exponential phase at the end of each experiment (n = 3). See Fig. 1 for definitions

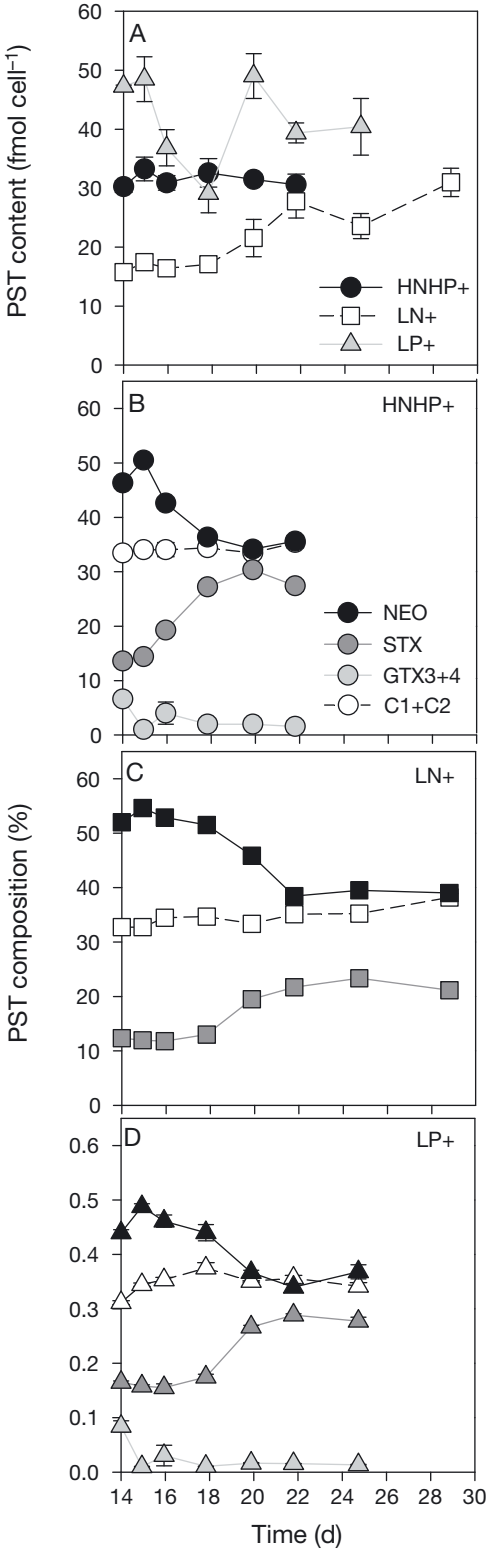

Fig. 5. *Alexandrium tamarense*. Changes (mean ± SE) in cellular paralytic shellfish poisoning toxins (PST) (A) content and (B–D) composition in the different treatments after transfer of cells into nutrient-replete medium on Day 14 (n = 3). NEO: neosaxitoxin; STX: saxitoxin; GTX: gonyautoxin. See Fig. 1 for other definitions

2002). After the transfer of these cultures into a fresh medium, cells immediately resumed growth towards maximum growth rates similar to those prior to the transfer (Fig. 1, Table 1). In the nitrogen- and phosphorus-starved cultures, nutrient resupply caused growth to resume after a lag phase of 4 and 1 d, respectively (Fig. 1). The elongated lag phase upon nutrient resupply to nitrogen-starved cells confirm earlier observations (Zhu & Tillmann 2012) and

Table 2. *Alexandrium tamarense*. Toxin composition in the different treatments and growth phases. Data of the high nitrogen and high phosphorus (HNHP), low nitrogen (LN) and low phosphorus (LP) treatments in the 1st incubations were obtained from Day 14. Data from HNHP+ and LN+ and LP+ treatments in the 2nd incubations were obtained from Days 22, 29, and 25, respectively (+: nutrient-replete modified K medium). Values: mean ± SD (n = 3). NEO: neosaxitoxin; GTX: gonyautoxin; STX: saxitoxin. [a–d]Significant differences between treatments and growth phases (ANOVA, $p < 0.001$, followed by Tukey's HSD, $p < 0.05$)

Treatment	C1+C2 (fmol cell^{-1})	GTX3+4 (fmol cell^{-1})	STX (fmol cell^{-1})	NEO (fmol cell^{-1})	C1+C2:Total (molar)	GTX3+4:Total (molar)	STX:Total (molar)	NEO:Total (molar)
First incubation, stationary phase								
HNHP	10.1 ± 0.4^{a}	2.02 ± 0.51^{a}	4.1 ± 0.3^{a}	14.0 ± 0.6^{ad}	0.33 ± 0.01^{ab}	0.07 ± 0.01	0.14 ± 0.01^{a}	0.46 ± 0.01^{a}
LN	5.2 ± 0.3^{b}	0.48 ± 0.57^{b}	1.9 ± 0.2^{b}	8.2 ± 0.2^{b}	0.33 ± 0.01^{ab}	0.03 ± 0.03	0.12 ± 0.01^{a}	0.52 ± 0.02^{b}
HN	14.7 ± 0.2^{c}	3.97 ± 0.87^{c}	7.8 ± 0.2^{c}	20.8 ± 0.3^{c}	0.31 ± 0.01^{a}	0.08 ± 0.02	0.17 ± 0.01^{b}	0.44 ± 0.01^{a}
Second incubation, exponential phase								
HNHP+	9.1 ± 2.6^{ab}	0.41 ± 0.13^{b}	7.2 ± 2.7^{acd}	9.2 ± 3.0^{ab}	0.35 ± 0.02^{b}	0.02 ± 0.01	0.27 ± 0.02^{c}	0.36 ± 0.01^{c}
LN+	11.8 ± 1.3^{a}	0.51 ± 0.12^{b}	6.6 ± 0.9^{acd}	12.1 ± 2.0^{abd}	0.38 ± 0.01^{bc}	0.02 ± 0.01	0.21 ± 0.01^{d}	0.39 ± 0.02^{c}
LP+	13.8 ± 2.8^{ac}	0.54 ± 0.09^{b}	11.3 ± 2.7^{d}	14.8 ± 2.9^{d}	0.34 ± 0.01^{ab}	0.01 ± 0.01	0.28 ± 0.01^{c}	0.28 ± 0.01^{c}

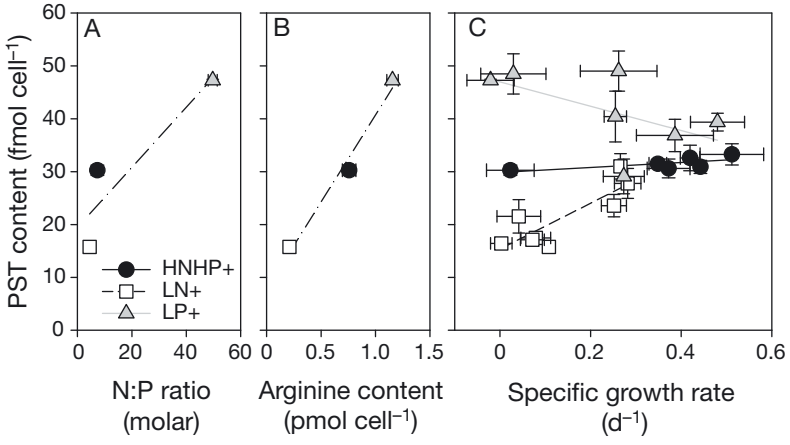

Fig. 6. *Alexandrium tamarense*. Relationship (mean ± SE) between paralytic shellfish poisoning toxins (PST) content and cellular (A) N:P ratios and (B) arginine content of nutrient-starved cultures, as well as between (C) PST content and the specific growth rate after the transfer of cells into nutrient-replete medium (n = 3). Lines show linear regressions. See Fig. 1 for definitions

clearly demonstrate a 'carry-over' effect of nitrogen starvation.

The maximum attained growth rates after nutrient resupply to phosphorus, but particularly to the nitrogen-starved cultures, were lower as compared to those measured prior to nutrient resupply. When phytoplankton are limited or starved by nitrogen, synthesis of nitrogen-rich cellular compounds, for instance proteins like transporters and enzymes, is typically reduced (Sterner & Elser 2002). This is also apparent from the lower amino acid content observed upon nitrogen starvation (Figs. 3 & 4). After resupply of nitrogen, the cellular nitrogen content fully recovered within 1 d, whereas full recovery of amino acid and PST contents seems much slower and lasted 4 and 8 d, respectively (Figs. 2–5). The slow recovery of the cellular amino acid content may explain the longer lag phase and possibly even underlie the lower achieved maximum growth rates. Starvation by phosphorus may cause a reduction of phosphorus-rich cellular compounds, such as ATP, nucleic acids, and phospholipids (Sterner & Elser 2002). Although synthesis of these cellular compounds after resupply of phosphorus seems insufficient for cells to immediately resume maximum growth, it is clearly faster than the resumed growth after nitrogen resupply to nitrogen-limited cells. Thus, the resource that limits growth determines the timing and rate at which *Alexandrium tamarense* will be able to resume growth and thus recover from nutrient-limited conditions.

After transfer of the cultures into a nutrient-replete medium, the cellular carbon and nitrogen contents increased 2- to 4-fold towards comparable values in all treatments (Fig. 2A–D). The relatively small changes in nitrogen quota upon a nitrogen pulse are in contrast to observations in cyanobacteria, which can store excess nitrogen in the polypeptide cyanophycin (Allen 1984, Van de Waal et al. 2010). *Alexandrium tamarense* seems incapable of such a luxury consumption of nitrogen and also cannot efficiently convert the sudden excess of nitrogen into biomass. The phosphorus content, however, showed a remarkable increase of up to 28-fold during the first 2 d after the transfer of phosphorus-starved cultures into the nutrient-replete medium (Fig. 2E). This luxury consumed phosphorus is presumably allocated to phosphorus-rich compounds such as polyphosphates that may serve as phosphorus storage (Fig. 7;

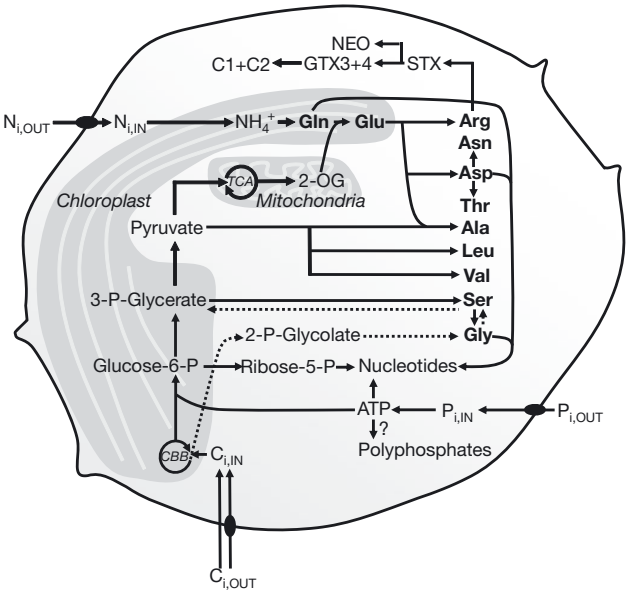

Fig. 7. Conceptual model of cell showing the coupling between assimilation of inorganic carbon (C_i), inorganic nitrogen (N_i) and inorganic phosphorus (P_i) with synthesis of amino acids and paralytic shellfish poisoning toxins (PSTs). CBB: Calvin-Benson-Bassham cycle; TCA: tricarboxylic acid cycle (i.e. citric acid cycle); 2-OG: 2-oxoglutarate. NEO: neosaxitoxin; GTX: gonyautoxin; STX: saxitoxin

Eixler et al. 2006, Nishikawa et al. 2006, Raven & Knoll 2010). The ability to rapidly take-up and store phosphorus (see also Yamamoto & Tarutani 1999), together with mixotrophic capabilities (Jeong et al. 2010) and the ability to use organic phosphorus (Anderson et al. 2012a, and references therein) may contribute to the widespread occurrence of *A. tamarense*. These traits provide a particular competitive advantage in waters with dynamically changing phosphorus concentrations (e.g. Smayda & Reynolds 2001). The tested *A. tamarense* strain was isolated from coastal North Sea waters (Alpermann et al. 2009, Tillmann et al. 2009), which indeed seem to be characterized by highly dynamic nutrient concentrations where phosphorus limitation may commonly occur (Loebl et al. 2009). To what extent these findings also apply to other *Alexandrium* species and strains needs to be further investigated.

Cells grown under nutrient-replete conditions showed the highest cellular amino acid content, followed by cells grown under phosphorus starvation. As expected, cells grown under nitrogen starvation comprised lowest amino acid content, confirming earlier findings with respect to *Alexandrium tamarense* (Figs. 3 & 4; Flynn et al. 1993). Once cells resumed growth after a 4 d lag phase, amino acid content increased and stabilized at values comparable to the other treatments (Fig. 3). Upon nutrient resupply to the nutrient-replete and phosphorus-starved cultures, the total amino acid content shows dynamic changes. This suggests that both nutrient limitation and resumed growth alter the cellular amino acid content. More specifically, the initial decrease in amino acid content might be a result of resumed growth, whereas the subsequent increase may be a result of recovery from nutrient limitation.

PST production is tightly coupled to the synthesis of amino acids, notably arginine (Shimizu 1996), which in turn depends on the carbon and nitrogen assimilation pathways (Fig. 7). The high amount of total amino acids under nutrient-replete conditions prior to the transfer can be largely explained by the high cellular glycine content (Fig. 4). In turn, this high cellular glycine content may be explained by enhanced photorespiration, which has been shown to be particularly promoted under low CO_2 conditions (Renberg et al. 2010). After the transfer into a fresh nutrient-replete medium, cellular glycine content dropped, whereas Glx content increased. Glx comprises first products in nitrogen assimilation (Fig. 7), and synthesis of glutamine was shown to be particularly promoted upon nitrogen resupply to nitrogen-limited cells of various dinoflagellate species (Flynn et al. 1993, 1996). Apparently, nitrogen assimilation was affected by the high pH, low CO_2 conditions in the nutrient-replete stationary cultures, and recovered upon transfer into a fresh nutrient-replete medium. Phosphorus limitation caused a shift in amino acid composition towards relatively more Glx and arginine. The higher cellular availability of arginine and its direct precursors, in turn, may explain the higher cellular PST content (Figs. 6 & 7, Table 1). Upon nutrient resupply to phosphorus-starved cells, cellular glycine content strongly increased. At the same time, cells contained only low amounts of valine and leucine (Fig. 4B). The lower cellular contents of these amino acids potentially resulted from enhanced synthesis of glycine. Production of glycine requires glyceraldehyde-3-phosphate, an important precursor for pyruvate, which in turn is needed for the synthesis of valine and leucine (Fig. 7). Thus, our results illustrate a tight coupling between assimilation of carbon, nitrogen and phosphorus, and the synthesis of amino acids and PSTs.

The cellular PST content and composition in *Alexandrium tamarense* showed differential changes after transfer into a nutrient-replete medium (Fig. 5). In the nutrient-rich treatment, PST content remained unaltered, whereas in the nitrogen-starved treatment it gradually increased (Fig. 5A). Interestingly,

in the phosphorus-starved cultures, PST content initially decreased until the third day, after which it rapidly returned to near maximal levels. This initial decrease in PST content occurred simultaneously with a substantial increase in cellular phosphorus content (Fig. 2D, E). The higher cellular phosphorus content caused a temporary decrease in the cellular N:P ratio. Under these conditions, cells potentially allocate nitrogen to the synthesis of phosphorus containing compounds, such as polyphosphates or nucleic acids (Fig. 7). As a result, this may lower the amount of nitrogen available for production of nitrogen-rich PSTs. Yet, the lowered PST content may also be associated with the enhanced growth rate occurring at the same time, which cannot be uncoupled from changes in N:P ratios. After the initial decrease, cellular PST content increased towards maximal values and was higher than observed in the nutrient-rich treatment. This suggests that phosphorus resupply to phosphorus-starved cells promoted the cellular PST content, which may be related to the seemingly higher cellular arginine content. Our results thus demonstrate a carry-over effect not only on growth, but also on PST content.

The cellular PST content has been shown to decrease upon nitrogen limitation or starvation, increase upon phosphorus limitation or starvation, and consequently increase with increasing cellular N:P ratios in various *Alexandrium* species (Table 3, Fig. 6A, see also Anderson et al. 1990a, Béchemin et al. 1999, John & Flynn 2000, Granéli & Flynn 2006, Lim et al. 2010, Murata et al. 2012). This relationship may be explained by shifts in amino acid content, particularly arginine (Table 3, Fig. 6B, see also Anderson et al. 1990a, Flynn et al. 1994, John & Flynn 2000). Yet, cellular PST content has also been shown to vary with growth rate. The direction of this change, however, depends on the growth-controlling nutrient. More specifically, when nitrogen controls growth, PST content typically increases with increasing growth rate. Contrastingly, when phosphorus controls growth, PST content typically decreases with increasing growth rate (Table 3, Fig. 6C, see also Anderson et al. 1990a,b, Cembella 1998, John & Flynn 1999, 2000, Leong et al. 2004, Lim et al. 2010). Here we show that upon nutrient starvation, PST content can be explained by the cellular N:P balance, and particularly by the cellular arginine content. Once nutrients are re-supplied, PST content can be related to growth rate, but the direction of this relationship depends on the growth-controlling nutrient (Fig. 6).

Besides changes in PST content upon the transfer of cells into a nutrient-replete medium, we also observed a clear change in PST composition (Fig. 5B–D). Interestingly, PST composition shifted in all treatments from NEO towards STX upon the transfer. Vice versa, it seems that upon growth limitation, irrespective of the limiting resource, part of the synthesized STX is hydroxylated towards NEO

Table 3. *Alexandrium* spp. Relative changes in total cellular paralytic shellfish poisoning toxins (PST) content of various reported *Alexandrium* spp. in response to N and P limitation or starvation (during stationary/steady state growth) compared to non-limiting conditions (exponential growth). Arrows: increase (↑) or decrease (↓) in cellular PST content upon nitrogen (LN) or phosphorus limitation (LP), and with increasing cellular/supply N:P ratios, growth rate, and amino acid content. (–): PST content did not change. Shift (Y) or no shift (N) in PST composition; na: not analysed

Reported species	Strain	LN conditions	LP conditions	N:P ratio	Growth rate LN	Growth rate LP	Amino acid content	Shift in PST composition	Reference
A. tamarense	NEPCC 255	↓	↑	na	na	na	na	N	Boyer et al. (1987)
	Pr18b	↓	na	na	na	na	na	Y	MacIntyre et al. (1997)
	Pr18b	–	na	na	–	na	na	Y	Parkhill & Cembella (1999)
	ATKR-020415	↓	na	na	↑	na	na	Y	Leong et al. (2004)
	ATKR-020415	↓	↑	↑	↑	↑	na	Y	Murata et al. (2012)
	Alex2	↓	↑	↑	↑	↓	↑	Y	This study
A. minutum	AM89BM	↓	↑	↑	na	na	na	Y	Béchemin et al. (1999)
	AL1V, AL2V	↓	↓	na	↑/–	↑/–	↑	na	Flynn et al. (1994)
	AL1V	na	↑	na	na	–	na	Y	Guisande et al. (2002)
	AmKB06	↓	na	↑	↑	na	na	Y	Lim et al. (2010)
A. fundyense	GtCA29	↓	↑	↑	↑	↓	↑/–	na	Anderson et al. (1990a)
	GtCA29	↓	↑	na	↑	↓	na	Y	Anderson et al. (1990b)
	CCMP 117	↓	na	na	↑	na	–	N	John & Flynn (1999)
	GtCA29	na	↑	na	na	↓	na	Y	Taroncher-Oldenburg et al. (1999)
	CCMP 1846	↓	↑	↑	↑	↓	↑	N	John & Flynn (2000)

(Fig. 7). Such a shift in PST composition has been reported earlier in *Alexandrium tamarense*, changing from STX towards NEO when cells reached stationary growth (Boczar et al. 1988). Furthermore, *A. tamarense* cultures grown under nitrogen-limited conditions produced relatively less STX and more NEO as compared to nitrogen-replete growing cultures (MacIntyre et al. 1997). Several other studies also reported comparable changes in PST composition of *A. tamarense* during the transition from exponential to stationary growth phase. For instance, PST composition shifted towards relatively less C2 and relatively more of the hydroxylated C4 (Hamasaki et al. 2001), or towards relatively less GTX5 and relatively more of the hydroxylated GTX1, GTX4 and GTX6 (Boyer et al. 1987). Thus, growth limitation as a result of nutrient stress may have consequences for the hydroxylation of PST analogues, although further work is needed to fully elucidate the processes underlying this relationship.

Here, we confirm earlier studies about the impact of nutrient availability on the cellular PST content in *Alexandrium* spp. When cells are starved, PST content and changes therein can be explained by N:P stoichiometry and arginine content. Once in exponential growth, PST content can be largely related to growth rate, but this relationship depends on the growth-controlling resource. Furthermore, resource limitation may promote hydroxylation of PSTs shifting the PST composition towards more NEO and less STX. Our findings also illustrate a high potential of luxury consumption of phosphorus by *A. tamarense*, which may contribute to its widespread occurrence. All in all, we show that linking carbon, nitrogen and phosphorus assimilation with amino acid synthesis improves our understanding of processes underlying the cellular PST content and composition.

Acknowledgements. The authors thank Y.-L. Chen and Y. Bublitz for assistance with the experiments, J. Hölscher and K.-U. Ludwichowski for performing the amino acid analyses, A. Müller for helping with the PST analyses, and S. Rokitta for his helpful comments. D.B.v.d.W., B.R., and U.J. thank BIOACID, financed by the German Ministry of Education and Research. Furthermore, this work was supported by the European Community's Seventh Framework Programme (FP7/2007-2013)/ERC grant agreement No. 205150 and contributes to EPOCA under the grant agreement No. 211384.

LITERATURE CITED

Allen MM (1984) Cyanobacterial cell inclusions. Annu Rev Microbiol 38:1–25

Alpermann TJ, Beszteri B, John U, Tillmann U, Cembella AD (2009) Implications of life-history transitions on the population genetic structure of the toxigenic marine dinoflagellate *Alexandrium tamarense.* Mol Ecol 18: 2122–2133

Anderson DM, Kulis DM, Sullivan JJ, Hall S (1990a) Toxin composition variations in one isolate of the dinoflagellate *Alexandrium fundyense.* Toxicon 28:885–893

Anderson DM, Kulis DM, Sullivan JJ, Hall S, Lee C (1990b) Dynamics and physiology of saxitoxin production by the dinoflagellates *Alexandrium* spp. Mar Biol 104:511–524

Anderson DM, Alpermann TJ, Cembella AD, Collos Y, Masseret E, Montresor M (2012a) The globally distributed genus *Alexandrium*: multifaceted roles in marine ecosystems and impacts on human health. Harmful Algae 14:10–35

Anderson DM, Cembella AD, Hallegraeff GM (2012b) Progress in understanding harmful algal blooms: paradigm shifts and new technologies for research, monitoring, and management. Ann Rev Mar Sci 4:143–176

Béchemin C, Grzebyk D, Hachame F, Hummert C, Maestrini SY (1999) Effect of different nitrogen/phosphorus nutrient ratios on the toxin content in *Alexandrium minutum.* Aquat Microb Ecol 20:157–165

Boczar BA, Beitler MK, Liston J, Sullivan JJ, Cattolico RA (1988) Paralytic shellfish toxins in *Protogonyaulax tamarensis* and *Protogonyaulax catenella* in axenic culture. Plant Physiol 88:1285–1290

Boyer GL, Sullivan JJ, Andersen RJ, Harrison PJ, Taylor FJR (1987) Effects of nutrient limitation on toxin production and composition in the marine dinoflagellate *Protogonyaulax tamarensis.* Mar Biol 96:123–128

Cembella AD (1998) Ecophysiology and metabolism of paralytic shellfixh toxins in marine microalgae. In: Anderson DM, Cembella AD, Hallegraeff GM (eds) Physiological ecology of harmful algal blooms, Book G41. Springer-Verlag, Berlin, p 281–403

Eixler S, Karsten U, Selig U (2006) Phosphorus storage in *Chlorella vulgaris* (Trebouxiophyceae, Chlorophyta) cells and its dependence on phosphate supply. Phycologia 45:53–60

Elser JJ, Bracken MES, Cleland EE, Gruner DS and others (2007) Global analysis of nitrogen and phosphorus limitation of primary producers in freshwater, marine and terrestrial ecosystems. Ecol Lett 10:1135–1142

Fitznar HP, Lobbes JM, Kattner G (1999) Determination of enantiomeric amino acids with high-performance liquid chromatography and pre-column derivatisation with o-phthaldialdehyde and N-isobutyrylcysteine in seawater and fossil samples (mollusks). J Chromatogr A 832: 123–132

Flynn K, Flynn KJ, Jones KJ (1993) Changes in dinoflagellate intracellular amino acids in response to diurnal changes in light and N supply. Mar Ecol Prog Ser 100: 245–252

Flynn K, Franco JM, Fernandez P, Reguera B, Zapata M, Wood G, Flynn KJ (1994) Changes in toxin content, biomass and pigments of the dinoflagellate *Alexandrium minutum* during nitrogen refeeding and growth into nitrogen or phosphorus stress. Mar Ecol Prog Ser 111: 99–109

Flynn KJ, Flynn K, John EH, Reguera B, Reyero MI, Franco JM (1996) Changes in toxins, intracellular and dissolved free amino acids of the toxic dinoflagellate *Gymnodinium catenatum* in response to changes in inorganic nutrients and salinity. J Plankton Res 18:2093–2111

Gotelli NJ (1995) A primer of ecology. Sinauer Associates, Sunderland, MA

Granéli E, Flynn K (2006) Chemical and physical factors influencing toxin content. In: Granéli E, Turner JT (eds) Ecology of harmful algae. Ecological Studies, Vol 189. Springer-Verlag, Berlin, p 229–241

Granéli E, Turner JT (2006) Ecology of harmful algae. Ecological Studies, Vol 189. Springer-Verlag, Berlin

Grasshoff K, Kremling K, Ehrhardt M (1999) Methods of seawater analysis. Wiley-VCH, Weinheim

Guisande C, Frangópulos M, Maneiro I, Vergara AR, Riveiro I (2002) Ecological advantages of toxin production by the dinoflagellate *Alexandrium minutum* under phosphorus limitation. Mar Ecol Prog Ser 225:169–176

Hamasaki K, Horie M, Tokimitsu S, Toda T, Taguchi S (2001) Variability in toxicity of the dinoflagellate *Alexandrium tamarense* isolated from Hiroshima Bay, western Japan, as a reflection of changing environmental conditions. J Plankton Res 23:271–278

Hansen PJ (2002) Effect of high pH on the growth and survival of marine phytoplankton: implications for species succession. Aquat Microb Ecol 28:279–288

Hansen HP, Koroleff F (1999) Determination of nutrients. In: Grasshoff K, Kremling K, Ehrhardt M (eds) Methods of seawater analysis. Wiley-VCH, Weinheim, p 159–228

Huisman J, Jonker RR, Zonneveld C, Weissing FJ (1999) Competition for light between phytoplankton species: experimental tests of mechanistic theory. Ecology 80: 211–222

Jeong HJ, Yoo YD, Kim JS, Seong KA, Kang NS, Kim TH (2010) Growth, feeding and ecological roles of the mixotrophic and heterotrophic dinoflagellates in marine planktonic food webs. Ocean Sci J 45:65–91

John EH, Flynn KJ (1999) Amino acid uptake by the toxic dinoflagellate *Alexandrium fundyense*. Mar Biol 133: 11–19

John EH, Flynn KJ (2000) Growth dynamics and toxicity of *Alexandrium fundyense* (Dinophyceae): the effect of changing N:P supply ratios on internal toxin and nutrient levels. Eur J Phycol 35:11–23

Keller MD, Selvin RC, Claus W, Guillard RRL (1987) Media for the culture of oceanic ultraphytoplankton. J Phycol 23:633–638

Krock B, Seguel CG, Cembella AD (2007) Toxin profile of *Alexandrium catenella* from the Chilean coast as determined by liquid chromatography with fluorescence detection and liquid chromatography coupled with tandem mass spectrometry. Harmful Algae 6:734–744

Leong SCY, Murata A, Nagashima Y, Taguchi S (2004) Variability in toxicity of the dinoflagellate *Alexandrium tamarense* in response to different nitrogen sources and concentrations. Toxicon 43:407–415

Lim PT, Leaw CP, Kobiyama A, Ogata T (2010) Growth and toxin production of tropical *Alexandrium minutum* Halim (Dinophyceae) under various nitrogen to phosphorus ratios. J Appl Phycol 22:203–210

Loebl M, Colijn F, van Beusekom JEE, Baretta-Bekker JG and others (2009) Recent patterns in potential phytoplankton limitation along the Northwest European continental coast. J Sea Res 61:34–43

MacIntyre JG, Cullen JJ, Cembella AD (1997) Vertical migration, nutrition and toxicity in the dinoflagellate *Alexandrium tamarense*. Mar Ecol Prog Ser 148:201–216

Murata A, Nagashima Y, Taguchi S (2012) N:P ratios controlling the growth of the marine dinoflagellate *Alexandrium tamarense*: content and composition of paralytic shellfish poison. Harmful Algae 20:11–18

Nishikawa K, Machida H, Yamakoshi Y, Ohtomo R, Saito K, Saito M, Tominaga N (2006) Polyphosphate metabolism in an acidophilic alga *Chlamydomonas acidophila* KT-1 (Chlorophyta) under phosphate stress. Plant Sci 170: 307–313

Nixon SW (1995) Coastal marine eutorphication: a definition, social causes, and future concerns. Ophelia 41: 199–219

Parkhill JP, Cembella AD (1999) Effects of salinity, light and inorganic nitrogen on growth and toxigenicity of the marine dinoflagellate *Alexandrium tamarense* from northeastern Canada. J Plankton Res 21:939–955

Quinn GP, Keough MJ (2002) Experimental design and data analysis for biologists. Cambridge University Press, Cambridge

Raven JA, Knoll AH (2010) Non-skeletal biomineralization by eukaryotes: matters of moment and gravity. Geomicrobiol J 27:572–584

Renberg L, Johansson AI, Shutova T, Stenlund H and others (2010) A metabolomic approach to study major metabolite changes during acclimation to limiting CO_2 in *Chlamydomonas reinhardtii*. Plant Physiol 154:187–196

Shimizu Y (1996) Microalgal metabolites: a new perspective. Annu Rev Microbiol 50:431–465

Shimizu Y, Norte M, Hori A, Genenah A, Kobayashi M (1984) Biosynthesis of saxitoxin analogs: the unexpected pathway. J Am Chem Soc 106:6433–6434

Sivonen K, Jones G (1999) Cyanobacterial toxins. In: Chorus I, Bartram J (eds) Toxic cyanobacteria in water: a guide to their public health consequences, monitoring and management. E & FN Spon, WHO, London, p 41–112

Smayda TJ, Reynolds CS (2001) Community assembly in marine phytoplankton: application of recent models to harmful dinoflagellate blooms. J Plankton Res 23: 447–461

Smith VH, Tilman GD, Nekola JC (1999) Eutrophication: impacts of excess nutrient inputs on freshwater, marine, and terrestrial ecosystems. Environ Pollut 100:179–196

Sterner RW, Elser JJ (2002) Ecological stoichiometry: the biology of elements from molecules to the biosphere. Princeton University Press, Princeton, NJ

Talling JF (1976) Depletion of carbon dioxide from lake water by phytoplankton. J Ecol 64:79–121

Taroncher-Oldenburg G, Kulis DM, Anderson DM (1997) Toxin variability during the cell cycle of the dinoflagellate *Alexandrium fundyense*. Limnol Oceanogr 42: 1178–1188

Taroncher-Oldenburg G, Kulis DM, Anderson DM (1999) Coupling of saxitoxin biosynthesis to the G1 phase of the cell cycle in the dinoflagellate *Alexandrium fundyense*: temperature and nutrient effects. Nat Toxins 7: 207–219

Tillmann U, Alpermann TL, da Purificacao RC, Krock B, Cembella A (2009) Intra-population clonal variability in allelochemical potency of the toxigenic dinoflagellate *Alexandrium tamarense*. Harmful Algae 8:759–769

Tonk L, Van de Waal DB, Slot P, Huisman J, Matthijs HCP, Visser PM (2008) Amino acid availability determines the ratio of microcystin variants in the cyanobacterium *Planktothrix agardhii*. FEMS Microbiol Ecol 65:383–390

Van de Waal DB, Verspagen JMH, Lurling M, Van Donk E, Visser PM, Huisman J (2009) The ecological stoichiometry of toxins produced by harmful cyanobacteria: an

experimental test of the carbon-nutrient balance hypothesis. Ecol Lett 12:1326–1335

Van de Waal DB, Ferreruela G, Tonk L, Van Donk E, Huisman J, Visser PM, Matthijs HCP (2010) Pulsed nitrogen supply induces dynamic changes in the amino acid composition and microcystin production of the harmful cyanobacterium *Planktothrix agardhii*. FEMS Microbiol Ecol 74:430–438

Welker M, von Döhren H (2006) Cyanobacterial peptides: nature's own combinatorial biosynthesis. FEMS Microbiol Rev 30:530–563

Yamamoto T, Tarutani K (1999) Growth and phosphate uptake kinetics of the toxic dinoflagellate *Alexandrium tamarense* form Hiroshima Bay in the Seto Inland Sea, Japan. Phycol Res 47:27–32

Zhu MM, Tillmann U (2012) Nutrient starvation effects on the allelochemical potency of *Alexandrium tamarense* (Dinophyceae). Mar Biol 159:1449–1459

Editorial responsibility: Toshi Nagata, Kashiwanoha, Japan

Submitted: April 16, 2013; Accepted: August 22, 2013
Proofs received from author(s): November 12, 2013